Trade-off analysis framework for PV-battery systems in multi-functional building complexes

A techno-economic assessment with real-world airport application

Yang, Xuesong; Zeng, Chao; Yao, Yushan; Luo, Jianing; Liu, Zhengxuan

DOI
10.1016/j.rineng.2025.107665

Publication date
2025

Document Version
Final published version

Published in
Results in Engineering

Citation (APA)
Yang, X., Zeng, C., Yao, Y., Luo, J., & Liu, Z. (2025). Trade-off analysis framework for PV-battery systems in multi-functional building complexes: A techno-economic assessment with real-world airport application. *Results in Engineering*, *28*, Article 107665. https://doi.org/10.1016/j.rineng.2025.107665

Results in Engineering 28 (2025) 107665

Contents lists available at ScienceDirect

Results in Engineering

journal homepage: www.sciencedirect.com/journal/results-in-engineering

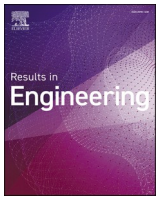

Trade-off analysis framework for PV-battery systems in multi-functional building complexes: A techno-economic assessment with real-world airport application

Xuesong Yang [a], Chao Zeng [b], Yushan Yao [c], Jianing Luo [b,*], Zhengxuan Liu [d,*]

[a] China Southwest Architecture Design and Research Institute Co. Ltd., Chengdu 610041, China
[b] School of Mechanical Engineering, Southwest Jiaotong University, Chengdu 610031, China
[c] Wuxi Hundun Energy Technology Co., Ltd., Wuxi 214000, China
[d] Faculty of Architecture and the Built Environment, Delft University of Technology, Julianalaan 134, 2628 BL, Delft, Netherlands

ARTICLE INFO

Keywords:
Techno-economic assessment
Multi-functional building complex
Solar energy application
Scoring-based evaluation
Levelized cost of energy
Renewable energy penetration

ABSTRACT

This study addresses the challenge of designing cost-effective and energy-efficient solar energy systems for large-scale, multi-functional building complexes, which typically exhibit high and diverse energy demands. Although integrating solar power with energy storage has shown promise, existing research rarely considers the full complexity of such building types or the trade-offs between cost and renewable energy use. To fill this gap, this study develops a novel assessment framework that quantitatively evaluates system performance across both energy and economic dimensions. The framework is applied to a real-world airport cargo terminal comprising ten functional zones, evaluating six system configurations with different photovoltaic areas and battery capacities. Two optimization objectives are considered: maximizing the share of energy supplied by solar generation and minimizing the levelized cost of electricity. The results show that two of the six configurations stand out as most representative: Case 3 adopts full rooftop and façade photovoltaics with an 87.94 MWh battery, enabling 60 % renewable energy penetration and the highest overall performance score of 4.6 (out of 6), though it requires 14.5 % higher investment; Case 5 uses only façade photovoltaics without storage, delivering the maximum cost saving of 10.4 % and the lowest energy cost of 0.49 CNY/kWh. The findings reveal a clear trade-off between maximizing renewable energy use and minimizing cost. This work contributes a novel, scalable framework for evaluating and optimizing solar energy systems in complex building environments, offering practical decision support for designers, policymakers, and investors seeking to promote sustainable urban energy transitions.

1. Introduction

Rising economic and environmental awareness, together with incentives from local governments, have catalysed a growing demand for renewable energy. Projections indicate that the proportion of renewable energy in total primary energy is expected to surge from 14 % in 2015 to 63 % by 2050, and in the power sector from 25 % in 2015 to 85 % by 2050 [1]. Among diverse renewable energy sources, solar energy systems, particularly those integrating photovoltaic (PV) panels into building rooftops and facades, are extensively deployed for heating, cooling, lighting, and electricity generation. This PV power generation systems is not only aesthetically appealing but also economically viable and technically sound [2]. The adoption of these PV systems, capable of fulfilling partial energy demands, could substantially reduce building energy costs and carbon emissions [3,4].

Building-integrated photovoltaic (BIPV) technologies are regarded as a commonly used promising solution to reduce building energy costs and carbon emissions, applicable to various types of buildings [5]. Previous research focusing on rooftop solar photovoltaic (PV) systems has attracted significant attention [6-8]. Luo et al. [9] found that 60 % of the PV energy penetration for the renewable energy system can

Abbreviations: BIPV, Building integrated photovoltaics; COP, Coefficient of performance; LCOE, Levelized cost of energy; MCDM, Multi-Criteria Decision Making; MAUT, Multi-Attribute Utility Theory; PLS, Peak load shedding; PV, Photovoltaics; REP, Renewable energy penetration; RPUE, Renewable power use efficiency; HVAC, Heating ventilation and air conditioning; IEA, The International Energy Agency; EBC, Energy in Buildings and Communities; TRNSYS, Transient System Simulation Program.

* Corresponding authors.
E-mail addresses: jianing.luo@connect.polyu.hk (J. Luo), Z.liu-12@tudelft.nl, zxliu626@hnu.edu.cn (Z. Liu).

https://doi.org/10.1016/j.rineng.2025.107665
Received 22 July 2025; Received in revised form 25 September 2025; Accepted 9 October 2025
Available online 10 October 2025

Nomenclature

A_{PV}	Total area of PV panels m^2
$C_{fac,k}$	The initial cost of the k^{th} facility CNY
$C_{tot,k}$	Total cost at the year k CNY
$C_{PV,k}$	Initial cost of the PV panels CNY
C_{Bat}	Initial cost of the battery storage CNY
C_{ic}	Annual income CNY/Y
C_{ei}	Annual extra investment CNY/Y
$C_{LCOE,real}$	Real levelized cost of energy CNY/kWh
$C_{LCOE,equ}$	Equivalent levelized cost of energy CNY/kWh
$Cap_{bat,min}$	Minimum battery capacity kWh
$Cap_{bat,max}$	Maximum battery capacity kWh
Du_{annual}	Calculation of the islanded mode duration hour
E_{tot}	Total energy consumption kWh
F_Y	Fuel expenditures in year kWh
I_Y	Initial cost CNY
K_{PV}	Temperature coefficient of the PV panels /
$Load^d_{peak,ref}$	Peak load in the reference case kW
$Load^d_{peak,ren}$	Peak load with renewable power generation kW
M_Y	Maintenance cost CNY
O_Y	Operation cost CNY
PS_{ave}	Average daily peak shedding kW
P^t_{grid}	Power charging from the main grids at the hour t kW
P_{PV}	Power generated from solar radiation kW
P^t_{con}	Power consumption kW
P^D_{peak}	Daily peak charging power kW
P^t_{tot}	Total load kW
$P_{ren,t}$	Renewable power generation in the production stage kW
Pr_{ele}	Current market electricity price CNY/kWh
$P_{ur,t}$	Total effectively-used renewable power consumption kW
Rad	Solar radiation per area W/m^2
R^d_{PLS}	Daily peak load shedding kWh
$R^D_{ocp,n}$	Occupancy rate %
$R_{batch,max}$	Maximum charging rate %
$R_{batdch,max}$	Maximum discharging rate %
T_{ref}	PV panels reference temperatures °C
T_{amb}	Ambient temperature °C
T_{ref}	Reference temperature °C
Y	Discount rate %
η_{PV}	Overall efficiency of PV panels %
η_{time}	Timely utilization ratio %
η_{ori}	The percent loss of solar energy production %

effectively achieve cost savings (up to 37.5 %). Lingfors et al. [10] pointed out that deploying PV only on the roofs of cultural-heritage buildings, with insolation > 900 kWh/m^2, results in a total PV yield of up to 2 % of the total electricity demand. Besides, with a particular focus on BIPV installations on rooftops, the vertical facades were also investigated as a supplement for PV utilization [11]. For example, in Rome, Italy, the deployment of the PV system across 60 % of the total surface area of the envelopes of 11 residential blocks has successfully met the criteria for near-zero energy consumption annually, despite the seasonal variations in energy production [12].

On the downside, the fluctuations of renewable power generation and building energy consumption can significantly affect both the system economic and energy performance [13]. Luo et al. [14] quantified the risk of power imbalance due to the fluctuations of renewable power generation and building energy consumption, where the highest hourly risk is quantified at about 4.8 % at 9:00 pm in a day. With the initiatives of IEA EBC Annex 67 [15], energy-flexibility service from buildings as an effective solution can be utilized to reduce surplus renewable energy [16]. Two general tendencies include energy storage and direct consumption by fully utilizing energy flexibility from the demand side [17, 18]. Battery storage, serving as an energy storage device, could store the peak electricity generated by PV and provide energy when electricity production is insufficient [19]. Particularly, the integration of an EV battery with a model predictive control system was developed and tested in a PV-based office building energy system [20]. The results indicated that this configuration could lead to a significant reduction in the levelized cost of energy (LCOE), achieving a potential improvement of up to 42.7 %. Similar studies [21-24] have proved that PV power generation together with battery storage has a promising potential to achieve cost savings and decrease carbon emissions.

To address the challenges posed by the intermittent and unpredictable natures of PV power generation, and to foster BIPV widespread adoption, it is essential to conduct accurate quantitative assessments and provide insightful analysis regarding the practical application of PV power generation [25]. Luo et al. [26] carried out a comprehensive quantitative assessment of BIPV applications on hotel roofs, demonstrating that an accurate assessment can effectively prevent the overestimation of extra charging power needs from the main grid, with a potential reduction of up to 70.6 %. Hu et al. [27] conducted a performance assessment of BIPV systems in Eastern China, concluding that they represent a promising solution for combined cooling, heating, and power generation, suitable for applications where electricity, heat, and cooling energy are all required. Besides, various studies have been conducted to quantitatively assess the performance of renewable energy systems, focusing on different types of buildings, including office buildings [28], residential houses [29], and hotel buildings [30]. Besides, a multi-functional building complex consists of multi-functional buildings in a determined area. Owing to its substantial energy demand, there is significant potential for reducing both energy consumption and carbon emissions through the implementation of renewable power generation [31].

In summary, BIPV systems are universally acknowledged for their significant potential to bolster economic, energy, and environmental sustainability [32]. Numerous comprehensive assessments have been conducted across various types of buildings, providing valuable insights into their applications and effectiveness [33]. Despite these advancements, the applications of BIPV systems in multi-functional building complexes is facing the following gaps:

- Firstly, actual implementation of BIPV systems in such complexes is rare, despite their considerable benefits.
- Secondly, a detailed and exhaustive evaluation of BIPV applications within multi-functional building complexes remains unavailable.
- Thirdly, the energy performance of BIPV systems in these complexes needs thorough quantification, taking into consideration the aggregated power consumption profiles of diverse functional buildings.

This entails fine-tuning the configuration of photovoltaic areas and battery storage capacities to guarantee efficient system integration and optimal performance. To address these challenges, this study proposes a comparative techno-economic assessment framework for PV power generation application in multi-functional building complexes. The framework is applied to a real-world case study of an international airport cargo terminal. The configurations of PV surface area and battery storage are optimized to achieve two competing objectives: maximizing renewable energy penetration (REP) and minimizing the levelized cost of electricity (LCOE). The main novelty of the proposed assessment approach and original contributions of this study are summarized as

follows:

- It proposes a zone-specific load modeling method that captures the detailed and dynamic energy characteristics of multi-functional building complexes;
- It develops a novel scoring mechanism for multi-criteria performance evaluation, integrating both energy and economic dimensions into a unified assessment framework;
- It demonstrates the practical feasibility of the proposed approach through a real-case study, providing actionable insights for energy system planning.

The structure of this paper is organized as follows. Section 2 presents the major procedure of the proposed quantitative assessment framework. Section 3 presents basic information of the multi-functional building complex and the developments of the model. Section 4 presents the results and analysis including the assessment of the multi-dimensional performance comparison. Section 5 presents the discussion and limitation. At last, Section 6 concludes the paper and future studies.

2. Methodology

2.1. Framework overview

Fig. 1 shows the framework of the proposed quantitative assessment approach, which consists of three steps. In this first step, power generation from solar energy and power consumption for the solar multi-functional building complex are calculated considering the different properties of the different function buildings. In the second step, the impacts of the PV area and battery capacity on the system performance are quantified. Then, the determination of the PV areas and battery capacities are conducted based on two different objectives; the maximum REP and the minimum LCOE. The last step provides the quantified techno-economic assessment results and analyzes the multi-dimensional performance comparisons. The details of these three steps are as follows,

- **Step 1**: In the first step, the characteristics of the multi-functional building complex are collected. Based on the determined building rooftops and building façades of the multi-functional building complex, the maximum available PV panel area is determined. The PV power generation is quantified based on the PV area, and PV power generation model together with the weather data. Then, as for demand, the working schedules of the equipment load for the multi-functional building complex together with their different energy densities such as equipment load density, light load density, and HVAC load density, are imported into the developed physical model. The physical model was created and simulated within a widely-used energy simulation software environment. Based on the mentioned model inputs as well as weather data, the different types of loads are calculated. The annual load profile is obtained, which is the sum of these loads.
- **Step 2:** The second step consists of two parts, i.e., system performance assessment and optimization of battery capacities and PV areas. Based on the determined ranges of the PV areas and battery capacities, the system performance is quantified. Then the optimization is conducted to obtain the optimized cases by maximizing REP and minimizing LCOE respectively.
- **Step 3:** In the third step, the multi-dimensional performance comparison is conducted. The assessment of the multi-dimensional performance comparison is based on several selected indicators, each quantified using established energy and economic performance indicators. The theoretical maximum total score for any configuration is determined by the number of assessment cases, while the minimum possible score is one. To ensure clarity and comparability, the average total score across all cases is used as the primary metric for subsequent assessment and analysis. Then based on the proposed new scoring mechanism for these cases, the recommended cases are obtained. As the outputs, this assessment approach and results can be

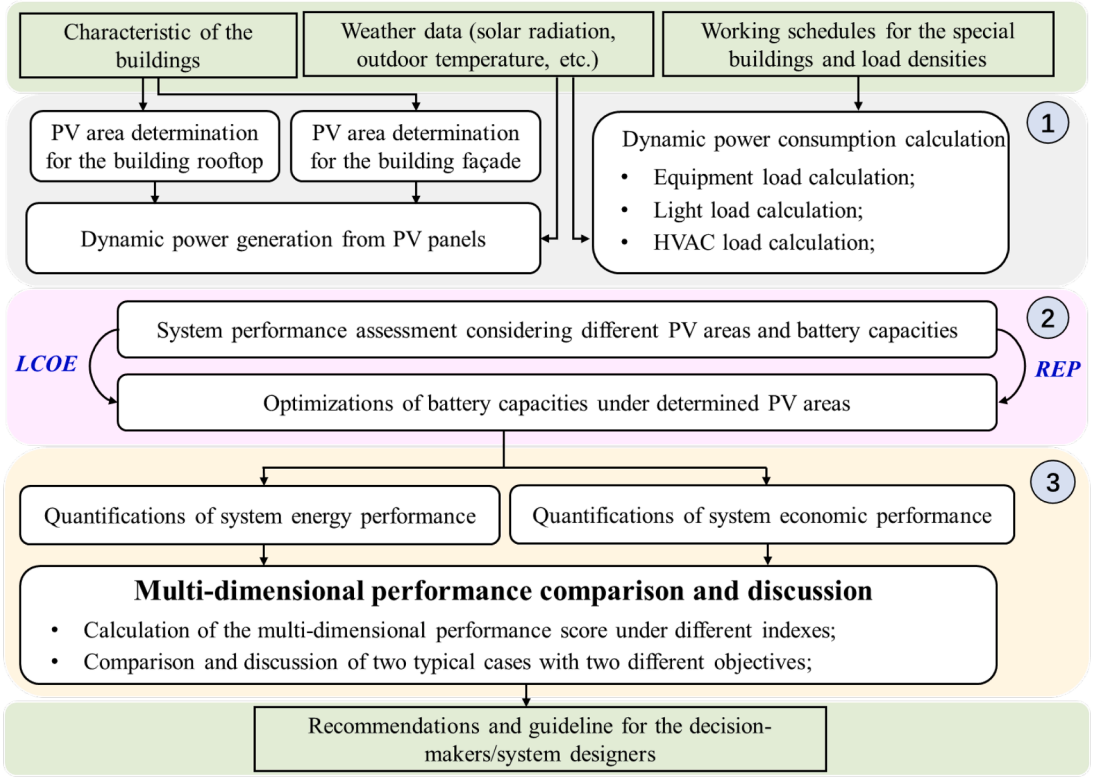

Fig. 1. The framework of the quantitative assessment approach.

used for the decision-makers and/or system designers as the guideline.

2.2. Energy performance quantification

2.2.1. Renewable energy penetration (REP)

The REP refers to the ratio of the total used renewable power generation ($P_{ur,t}$) to the hourly total electrical load (P_{tot}) as shown in Eq. (1) [34]. If the ratio is close to one, more demand can be met by renewable power generation. It is used as the objective function, where the direction of the optimization is to increase the REP. It is noted that since the typical year is taken into account, the up limit of t equals 8760 h.

$$REP = \sum_{t=1}^{t=8760} P_{ur,t} \Big/ \sum_{t=1}^{t=8760} P_{tot,t} \tag{1}$$

2.2.2. Renewable power use efficiency (RPUE)

The RPUE is used to quantify the generated power use efficiency from renewable sources [26], where $P_{ren,t}$ is the total renewable power generation. If the ratio is close to one, the generated renewable power is all used by the system.

$$RPUE = \sum_{t=1}^{t=8760} P_{ur,t} \Big/ \sum_{t=1}^{t=8760} P_{ren,t} \tag{2}$$

2.2.3. Grid impact indicators

The power grid impact indicators consist of the peak shedding and islanded mode duration. The former shows the average daily peak shedding and the latter measures the time when the system operates without support from the main girds (i.e., islanded mode duration), where the details of the calculation are presented as follows.

- **Peak shedding** is the reduction of the daily peak load when renewable power generation is considered in the system to meet the demand as a priority [35]. Eq. (3) is used to calculate the average daily peak shedding (PS_{ave}) [36].

$$PS_{ave} = 1/D \sum_{d=1}^{d=D} \left(Load^{d}_{peak,ref} - Load^{d}_{peak,ren} \right) \tag{3}$$

where, D is the number of days taken into account, $Load^{d}_{peak,ref}$ is the peak load in the reference case and $Load^{d}_{peak,ren}$ is the peak load with the renewable power generation consideration at day d, respectively.

- **Islanded mode duration** is the duration of the system operating without support from the main girds where the hourly power generated from the renewable is sufficient to meet the demand. Eq. (4) is used to calculate the islanded mode duration (Du_{annual}).

$$Du_{annual} = Du_{annual} + 1, \ if \ P^{t}_{grid} = 0 \tag{4}$$

where, P^{t}_{grid} is the power charging from the main grids at the time t. If the islanded mode duration is longer, the system is more independent. Besides, the longer islanded mode duration can effectively decrease the dependency of the system on the main grids, which can effectively avoid the outage risk due to the outage from the main grids and decrease the burden of the power charging from the main grids.

2.3. System economic performance quantification

2.3.1. Total system cost

The overall cost of the system consists of three major parts, i.e., the initial cost, the operating cost, and the maintenance cost (Eq. (5)). Note that, the overall costs of the system during the typical year are adopted in the system economic performance quantification considering different lifetimes (Y) of the electrical facilities. For instance, the lifetimes of PV panels and the battery are 20 years and 15 years, respectively, considering the properties of the different electrical components. The initial cost of the system (I_Y) is the sum of the annual initial cost of the PV panels ($C_{PV,k}$) and the battery storage (C_{Bat}), as shown in Eq. 7. The operation cost (O_Y) is the sum of the payment for the electricity purchase from the main grids, as shown in Eq. 8.

$$C_{ov} = I_Y + O_Y + M_Y \tag{5}$$

$$I_Y = \left(C_{PV,k} \times 1 \,/\, Y_{PV} \right) + \left(C_{Bat,k} \times 1 \,/\, Y_{Bat} \right) \tag{6}$$

$$O_Y = \left(\sum_{t=1}^{8760} P^{t}_{grid} \times \ \Delta t \right) \ \times Pr_{ele} \tag{7}$$

where, Pr_{ele} is the current market electricity price. The maintenance cost (M_Y), as shown in Eq. (8), is the annual maintenance cost that is used to support the maintenance of the major components of the renewable power generation system per year, which is about 1 % of the initial cost [37].

$$M_Y = 1\% \ \times \ \left(C_{PV,k} \times 1 \,/\, Y_{PV} + C_{Bat,k} \times 1 \,/\, Y_{Bat} \right) \tag{8}$$

2.3.2. Levelized cost of energy (LCOE)

In conventional evaluation methods, the economic value of the system is assessed using $LCOE_{con}$, which represents the price per energy unit (in CNY/kWh) that balances out all the costs associated with the system [38]. Eq. (9) shows the calculation process.

$$LCOE_{con} = \sum_{Y=1}^{Y} \frac{I_Y + O_Y + F_Y}{(1+r)^{Y}} \Big/ \sum_{t=1}^{n} \frac{E_Y}{(1+r)^{t}} \tag{9}$$

where, Y is the discount rate (%) and r the is degradation factor, I_Y is the initial cost expenditures in year Y, O_Y is the annual operation cost in year Y, and F_Y is the fuel expenditures in year Y. The F_Y is zero since the system uses no fossil fuels to generate electricity or meet demand. In the following calculation, r is the average value and is assumed to be 0.5 % [39] over the entirety of the lifetime because the computed LCOE is based on the usual year. Besides, the annual maintenance cost (M_Y) is also considered in this study. Thus, the calculation of the LCOE is modified and presented in Eq. (10).

$$LCOE = \left(\frac{I_Y + O_Y + M_Y}{(1+r)^{Y}} \right) \Big/ \left[E_0 \times (1 + r/100)^{Y} \right] \tag{10}$$

Additionally, the total power consumption (E_0) is calculated based on the hourly total electrical load ($P_{tot,t}$) as shown in Eq. (11).

$$E_0 = \sum_{t=1}^{t=8760} P_{tot,t} \tag{11}$$

3. Model development for the multi-functional building complex

3.1. Case study description

The developed assessment framework is applied to the typical multi-functional building complex, i.e., a cargo terminal situated in a western Chinese city at N30°28′, E104°49′, serving an international airport with a total size of 0.72 million square meters. The cargo terminal, which is depicted in Fig. 2, includes the 10 different building in three different areas (cargo area, living area and office area). The integrated system schematic featuring battery storage and photovoltaic generation has been shown for retrofitting the existing multifunctional complex in

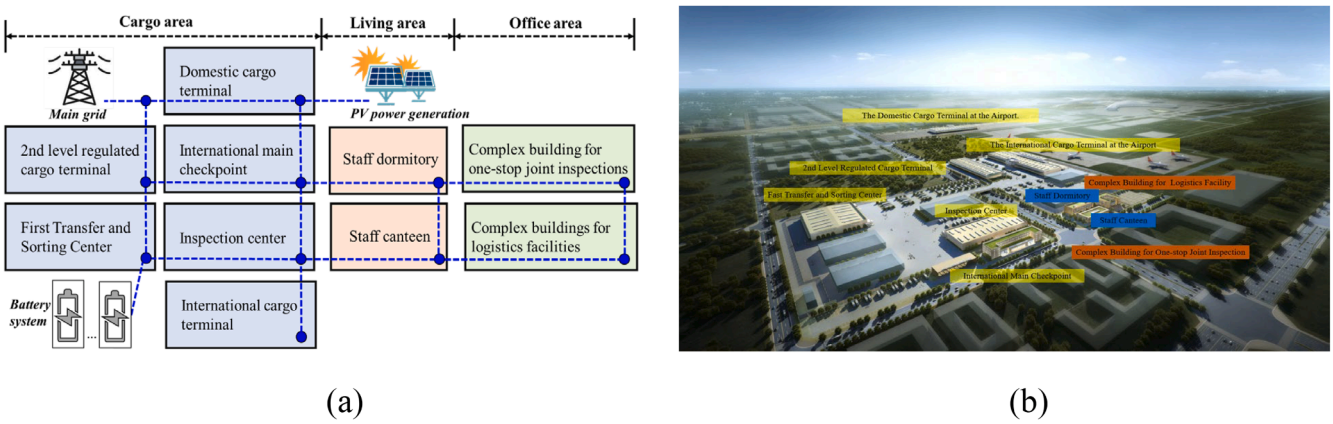

Fig. 2. Aerial view of the airport cargo terminal for system schematic diagram (a) and master plan visualization (b).

Fig. 2(a), while Fig. 2(b) illustrates the master plan visualization. This developed assessment approach was tested and validated based on an actual case study; therefore, the selection of the location did not involve extensive deliberation. The location from the actual case was adopted, and relevant cost data were derived from real-world pricing at the project destination.

The cargo terminal is a typical multi-functional building complex, which consists of three different functional areas. A total of ten functional building areas are involved in this study. The details of the basic information of the cargo terminal are presented in Table 1 and the load profile quantification for the cargo terminal is presented in Section 4.1.

Table 2 gives the cost data of the energy system, including the PV panels and battery, the unit prices, and their lifetimes. The unit price is determined by the current price, which is the sum of the installation price and the unit price. The value of the unit price of the electricity is taken according to the official electricity price in Sichuan (a western province of China).

Table 1
Basic information of the multi-functional building complex (airport cargo terminal).

Partition		Building area (m^2)	Roof area (m^2)	Façade area (m^2)	Floors (/)	Height (m)
Cargo area	Domestic cargo terminal	25,871	8623	6028	3	15.3
	International cargo terminal	31,861	10,620	9531	3	21.8
	2nd level regulated cargo terminal	12,996	6498	4480	2	13.1
	Fast transfer and sorting center	13,007	6503	5269	2	15.4
	Inspection center	10,670	5335	4091	2	13.2
	International main checkpoint	662	662	939	1	8.6
Office area	Complex buildings for logistics facilities	5746	1436	2830	4	17.6
	Complex building for one-stop joint inspection	11,300	2825	3969	4	17.6
Living area	Staff dormitory	2754	1377	1811	2	11.5
	Staff canteen	2754	1377	1811	2	11.5

Table 2
Cost data of the energy system[a].

Parameters	Value	Unit
The unit price of PV	1000	CNY/m^2
The unit price of the battery	800	CNY/kWh
The unit price of electricity	0.5464	CNY/kWh
Lifetime of PV	20	Year
Lifetime of battery	15	Year

Remark: the selection of reference data refer to Refs [40-42]

3.2. Load characteristics by functional zone

The load characteristic of a cargo terminal is generally higher than conventional buildings due to its operations and functions. In such a multi-functional building complex, heavy-duty equipment like cranes, conveyor belts, and forklifts are used to load and unload cargo, accounting for a significant amount of power consumption. Additionally, the terminal may also require specialized facilities like temperature-controlled storage areas and security systems.

The international airport cargo terminals are generally built in the plain areas. The building has a small height and a larger surface area. The large surface area provides an opportunity to take advantage of abundant sunlight. Solar energy can be efficiently and effectively used as a renewable energy source for the power supply.

The power consumption commonly consists of power consumption of the equipment, lighting, and HVAC load. The required equipment and lighting load on the demand side is determined by the terminal electricity power (*Pterm*), load time schedules (f), and the timely utilization ratio (η_{time}), which is defined by Eq. (12).

$$Lre = Pterm \times f \times \eta_{time} \tag{12}$$

The HVAC load is calculated according to the cooling load density and weather data. In the current planning stage of this project, specific chiller and corresponding water pumps have not yet been selected. Without detailed equipment performance data, introducing a dynamic COP model might introduce additional uncertainty rather than improve accuracy, as it would rely on generalized assumptions rather than actual unit characteristics [43]. To simplify calculation for this system-level feasibility study, the coefficient of performance (COP) of the cooling and heating equipment is assumed to be a constant value of 3.29 (summer)/ 3.67 (winter) [9]. TRNSYS, a commonly used demand-side dynamic simulation software, is used to simulate the power consumption of the HVAC load [44]. A key aspect of its functionality involves the calculation of building energy loads. Input parameters such as lighting load density, equipment load density, and cooling load density are supplied to the "TYPE 56″ module, which is tailored for detailed multi-zone building energy simulation. This module accurately models

solar radiation and heat transfer through windows, even in buildings with complex geometries. It also incorporates various heating, cooling, and ventilation configurations, delivering comprehensive outputs including system variables and energy consumption data [45]. Based on these simulations and specific weather conditions, TYPE 56 generates corresponding electrical load profiles for the buildings, providing essential data for energy system analysis and optimization.

3.3. Power generation by PV panels

Power generation by PV panels is used as a sustainable power supply. According to the dynamic solar radiation (*Rad*), the power generation is calculated using Eq. (13) [46]. The cell temperature (T_{PV}) has a significant impact on the power generation, which is calculated based on the ambient temperature (T_{amb}) and solar radiation, as shown in Eq. (14). Note that the overall efficiency of PV panels (η_{PV}) is set as 20 % [46].

$$P_{PV} = Rad \times A_{PV} \times \left(1 + K_{PV}\left(T_{PV} - T_{ref}\right)\right) \times \eta_{pv} \tag{13}$$

$$T_{PV} = T_{amb} + 0.0256 \times Rad \tag{14}$$

$$0 \le P_{PV,t} \le P_{PV}^{Max}, \ \forall t \in [1, 8760] \tag{15}$$

where, A_{PV} is the area of PV panels. T_{ref} is the reference temperature and it is set as 25 °C. K_{PV} is the temperature coefficient of the PV panels and it is set as -3.7×10^{-3} [14].

Since the installed PV panels are not only located on the rooftop but also on the façade, the percent loss of solar energy production (η_{ori}) per PV unit surface area considering the impact of the façade orientation is quantified and involved in the renewable power generation as shown in Eq. (16). Based on empirical practice, this value is often approximated as 20 %. To further refine the approach, data from relevant literature were synthesized to obtain more detailed information, which was used to enhance the subsequent PV power generation modelling and simulation. The percent loss of solar energy production for different façade orientations is defined according to the literature [12], where the maximum percent loss is 37 % for the north façade and the average percent loss is about 18.75 %.

$$P_{PV,fa} = P_{PV} \times \eta_{ori} \tag{16}$$

3.4. Determination of the PV areas and battery storage capacity for the cargo terminal energy system

3.4.1. PV area determination

According to the basic information of the cargo terminal, three scenarios concerning the different areas of the PV panels are shown in Table 3. In Scenario 1, the total area of the building rooftops is used to install the PV panels. In Scenario 2, the total area of the building façades is used to install the PV panels. In the last scenario, both facades and building rooftops are used to install the PV panels. These three typical scenarios concerning different capacities of the battery are used to quantify the system performance. Then the optimizations for the battery capacities are conducted based on these determined PV areas.

3.4.2. Battery storage capacity

The battery storage is used to store surplus electricity from PV and further increase renewable power use efficiency [47]. Under the estimated peak load (i.e., 3664 kW), the battery capacity, ranging from zero to 24-h storage of the hourly peak demand is considered and adopted in this work, as shown in Table 4. Note that the use of MWh for battery capacity is appropriate given the large scale of the energy storage system required for the multi-functional building complex. The impacts on the system energy and economic performance are further quantified and assessed comprehensively for a wide range of battery storage capacity.

Table 3
Summary of the scenarios for different PV areas.

Scenario	Rooftop	Façade	Total available area
PV_Scenario 1	Yes	No	45,256 m^2
PV_Scenario 2	No	Yes	40,756 m^2
PV_Scenario 3	Yes	Yes	86,012 m^2

3.5. Battery working principle and system control mechanism

The overall charge and discharge efficiencies are both set to 0.85 to simplify the calculation [48]. According to Eqs. (17) and (18) [49], the maximum hourly charging rate ($R_{batch,max}$) and hourly discharging rate ($R_{batdch,max}$) are set at 20 % and 50 % of the battery capacity, respectively, to ensure that the battery storage operates within a safe range [48]. According to Eq. (19), the minimum limit ($Cap_{bat,min}$) and maximum limit ($Cap_{bat,max}$) of battery capacity are set as 20 % and 85 %, respectively. Provided that the specified operating conditions are fulfilled, the battery is expected to function reliably throughout its entire design life of 15 years.

$$0 \le R_{batch} \le R_{batch,max} \tag{17}$$

$$0 \le R_{batdch} \le R_{batdch,max} \tag{18}$$

$$Cap_{bat,min} \le Cap_{bat} \le Cap_{bat,max} \tag{19}$$

To increase the system dependability and maintain the system functioning, an appropriate system control mechanism is required. Two typical modes of system operation mechanism are adopted, as indicated in Fig. 3, in accordance with solar energy generation, power charging from main grid, battery working principle, and power consumption. At the beginning, the mode determination is conducted. If the power consumption of the cargo terminal exceeds the amount of renewable power generation, Mode I is adopted. The power generation from PV panels as the first choice is used to meet the demand. Battery storage serves as a backup to supply the system with electricity until it exhausts its power reserves when solar energy production falls short of meeting immediate energy demand. The demand can be satisfied by utilizing the main grid if the battery cannot meet the demand (grid-connected mode adoption). If the generated electricity by PV panels is greater than the demand, Mode II is adopted. Only renewable energy is used for the power supply. The battery storage holds the extra electricity produced by renewable energy sources until it reaches its rated capacity. When the supply of renewable energy exceeds the demand and the battery storage is fully charged, the surplus electricity must be safely discarded (curtailed) to maintain system stability. This is a standard practice for ensuring reliable operation in renewable energy systems.

Table 4
Determination of the battery capacity range.

Number	Fully discharging duration T_{dis}	Battery capacity Cap_{bat}
1	0 h	0 MWh
2	2 h	7.33 MWh
3	4 h	14.66 MWh
4	6 h	21.98 MWh
5	8 h	29.31 MWh
6	10 h	36.64 MWh
7	12 h	43.97 MWh
8	14 h	51.30 MWh
9	16 h	58.62 MWh
10	18 h	65.95 MWh
11	20 h	73.28 MWh
12	22 h	80.61 MWh
13	24 h	87.94MWh

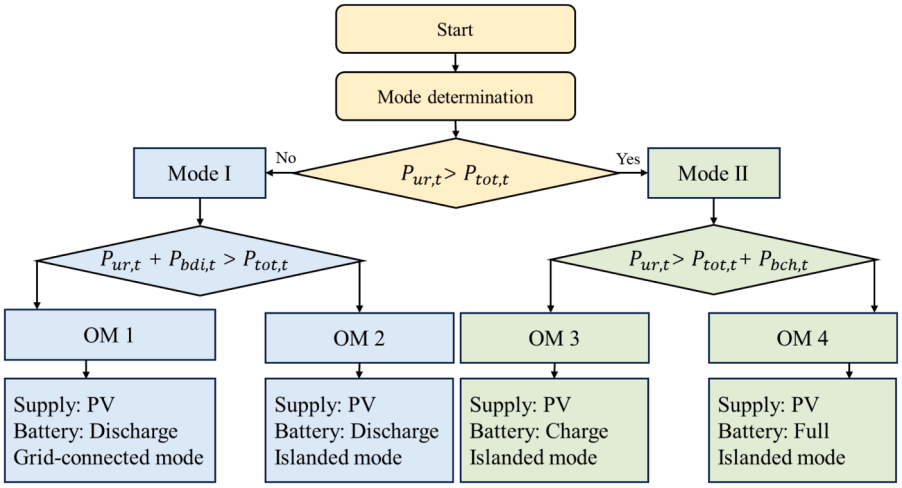

Fig. 3. Logical flowchart of the system control mechanism.

4. Results and analysis

4.1. Load profile quantification

Fig. 4 shows the power consumption for equipment and lighting in three parts: cargo area, office area, and living area, as shown in Table 1. Power consumption in office and living areas fluctuates with work schedules, similar to typical buildings. In the cargo area, natural light is often limited due to cargo stacking. A simple rule-based control is used for lighting to maintain stable power consumption during specific periods, despite actual variations. The power data combines measurements and assumptions to reflect realistic operating conditions. The equipment load shows a constant value at around 4500 kW throughout the 24-hour cycle. The power consumption for the office area and living area varies according to the working schedule similar to other public buildings.

Fig. 5 shows the cooling and heating load of the HVAC for three areas (i.e., cargo area, office area, and living area). Meteorological Data is input to TRNSYS to calculate the cooling and heating loads during the typical year. Note that only the cooling season and heating season are counted when the power consumption is calculated according to Section 3.2.

4.2. Impacts of the PV area and battery capacity and their optimizations

4.2.1. Levelized cost of energy (LCOE)

Fig. 6 shows the quantification results of the LCOE considering the determined three scenarios of the PV areas with different battery capacities. When the PV panels are solely installed on the building rooftops (Scenario 1), the LCOE decreases lightly at the beginning and increases gradually with the increase of the battery capacity. When the PV panels

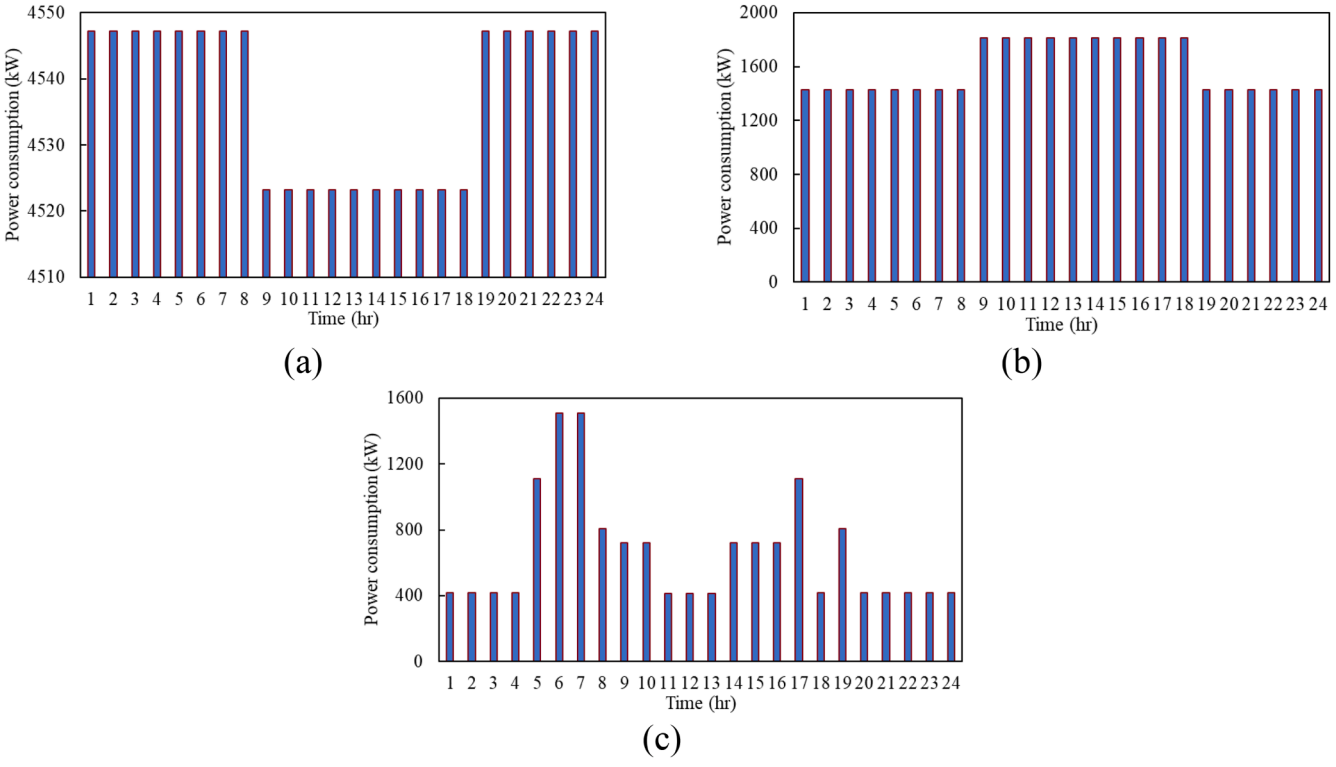

Fig. 4. Power consumption for equipment and lighting in three areas: (a) cargo area, (b) office area, and (c) living area.

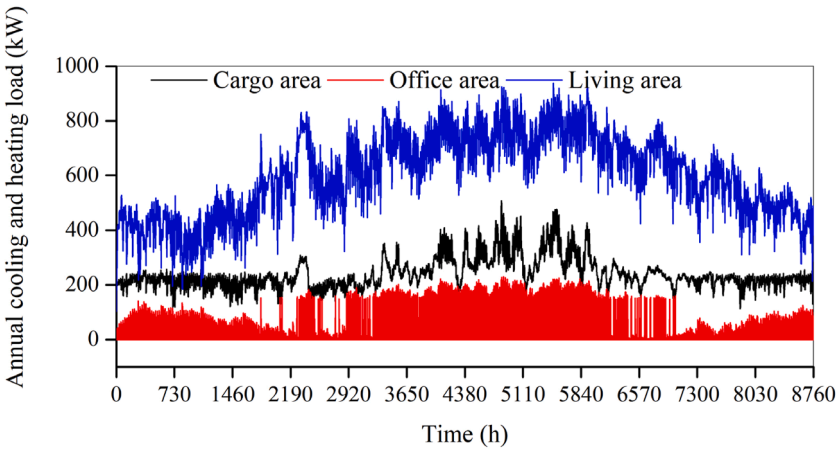

Fig. 5. Cooling and heating loads on the demand side for HVAC in the different areas.

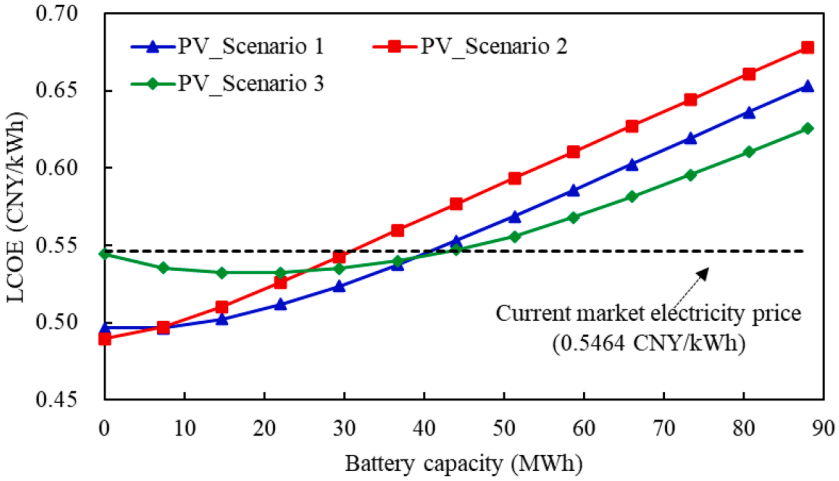

Fig. 6. Quantification results of the levelized cost of energy (LCOE) considering the determined three scenarios of the PV areas with different battery capacities.

are solely installed on the building façades (Scenario 2), the LCOE increases directly with the increase of the battery capacity. In this scenario, the LCOE is the lowest (i.e., 0.49 CNY/kWh) compared to the other scenarios where the battery is not adopted. As for Scenario 3, the PV panels are installed on both rooftops and façades, where the lowest LCOE is for the case of 21.98 MWh of the battery capacity. It indicates that increasing battery capacities may lead to a large LCOE, and the LCOE can even be higher than the current market electricity price (the black dash line as shown in Fig. 6). The selected proper battery capacity can effectively decrease the LCOE, and battery capacity should be optimized necessarily according to the specific PV area.

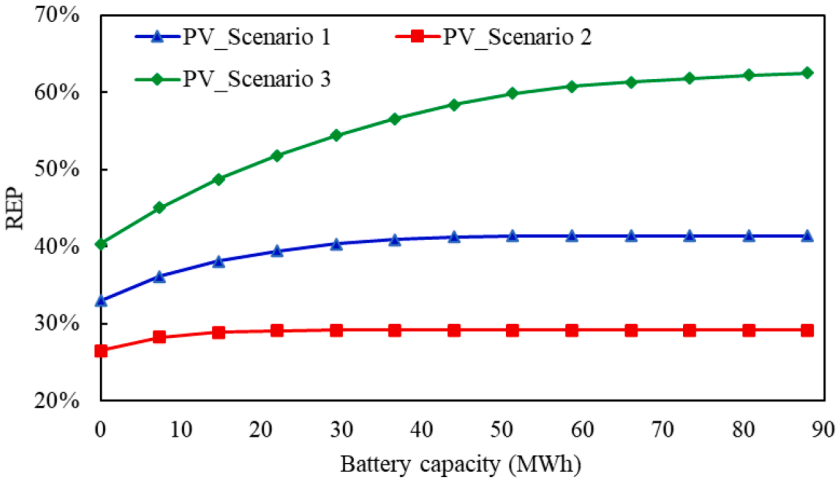

Fig. 7. Quantified results of the renewable energy penetration considering the determined three scenarios of the PV areas with different battery capacities.

4.2.2. Renewable energy penetration (REP)

Fig. 7 shows the REP quantification results considering three PV areas (i.e., three scenarios) under different battery capacities. It can be seen that the REP increases gradually and then becomes constant with the increase of the battery capacity. It indicates that enlarging the battery capacity is an effective method to increase the REP of the system but excessive battery capacity cannot increase the REP anymore. Specifically, a larger PV area leads to a larger REP, where the largest REP is up to 60 % in Scenario 3. The saturation occurs mainly because the PV area has reached its maximum practical limit. While increasing battery size could enhance energy shifting, further expansion does not increase REP. Hence, the limitation stems primarily from PV area availability, not battery capacity or curtailment. In addition, the best REP performance is achieved with different battery capacities in these three scenarios. To achieve the largest REP, the battery capacities are recommended as 65.95 MWh, 29.31 MWh, and 87.94 MWh for Scenario 1, Scenario 2, and Scenario 3, respectively. As a result, when the PV areas are determined, conducting the optimization of the battery capacities is a necessary solution to achieve the largest REP.

4.2.3. Optimizations for battery capacity

A total of six cases are presented in Table 5 concerning the mentioned two objectives (REP and LCOE) with three determined PV areas. The first three cases aim to maximize REP, and the calculated battery capacities are larger than the last three cases since increasing the battery capacity is an effective approach to increase the REP under certain circumstances. The last three cases aim to minimize LCOE, so the extra battery capacity is not involved. Since the extra initial cost of the battery capacity is considered in the optimization, the last three cases prefer to use smaller battery capacities and even zero (such as in Case 5). These six cases are further considered in the following comparative assessment and analysis.

4.3. Quantitative assessment results of the multi-functional building complex

4.3.1. Renewable power use efficiency (RPUE)

The quantified results of the RPUE among these six cases are presented in Fig. 8. The first three cases that aim to increase REP have better performance and even the first two cases are above 98 %. This is because these three cases have selected larger capacities of the batteries and the large battery can effectively increase the renewable power use efficiency by storing surplus renewable power generation instead of directly abandoning the electricity from PV panels. Without considering the energy performance in the optimization, the system performance of the RPUE in the last three cases is not satisfied, although their RPUE appears to be above 75 %. From this perspective, the first three cases especially the first two cases are better selections.

Table 5
Summary cases of the optimized battery capacity under three determined PV areas.

	Objective direction	Locations of the PV installation	PV area	Battery capacity
Case 1	Maximize REP	Rooftop	45,256 m^2	65.95 MWh
Case 2	Maximize REP	Façade	40,756 m^2	29.31 MWh
Case 3	Maximize REP	Rooftop and Façade	86,012 m^2	87.94 MWh
Case 4	Minimize LCOE	Rooftop	45,256 m^2	7.33 MWh
Case 5	Minimize LCOE	Façade	40,756 m^2	0.00 MWh
Case 6	Minimize LCOE	Rooftop and Façade	86,012 m^2	21.99 MWh

4.3.2. Import of energy from main grid

Additionally, two indicators (i.e., peak shedding and islanded mode duration) are taken into account to evaluate the effects on the import of energy from the main grid. The system performance of these two indicators is quantified and presented in Fig. 9. The peak shedding is presented as the bar charts of the primary y-axis and the islanded mode duration is shown in star points of the secondary y-axis. Among these six cases, Case 3 has the best performance for both two indicators, where the islanded mode duration is up to 55.3 % of the total hours and the average daily peak shedding is over 24 times than the worst case (Case 5). This is because the largest PV area and battery capacity are used in Case 3.

4.4. Assessment and comparison results of the system economic performance

Fig. 10 shows the assessment and comparison results of the system economic performance among these six cases. The blue dashed line represents the baseline of 0 % cost saving in Fig. 10. The cost results are presented as the bar charts of the primary y-axis and the comparison ratios are shown in star points of the secondary y-axis. If the cost saving is positive, it indicates that the cost saving is achieved. If the cost saving is negative, the extra cost is needed in the corresponding case. Among these six cases, the cost savings in the first three cases are negative. Since they are obtained via optimization to maximize REP while the LCOE is ignored. Higher LCOE values occur when PV or storage systems are poorly sized, increasing costs instead of saving money. This shows why energy projects must be carefully evaluated and optimally designed early in the planning phase. The last three cases are obtained via optimization to minimize LCOE, so the maximum cost saving is up to 10.4 % in Case 5. As a result, if the decision-makers and/or system designers solely focus on system economics, Case 5 is the optimum choice.

4.5. Multi-dimensional performance comparison and recommendations

Multi-dimensional performance comparison and the average score of the system performance among these six cases are presented in Fig. 11. A total of six cases are included in the assessment so the maximum score for each dimension is set to 6. Based on the five selected indicators, which were quantified according to previously established energy and economic performance metrics, the highest possible total score for any case is 30 points, while the lowest is 5 points. To facilitate clear interpretation of the results, the average total score across all cases is used for subsequent assessment and analysis. As for the scoring mechanism if the best performance in one dimension of one case appears, the full score (i.e., 6) is obtained in this dimension of this case. For instance, the highest REP is achieved in Case 3, and the full score in this dimension is obtained in this case. As for the five-dimensional performance comparison, Case 3 obtained the highest average score at 4.6. If the five-dimensional performance is equally important, Case 3 is recommended.

4.6. Power generation and load profiles during a typical week based on two recommended cases

This section directly depicts the difference between the recommended Case 3 and Case 5, where the former is recommended due to its highest score and the latter is recommended due to its largest cost saving. Fig. 12(a) and Fig. 12(b) show the weekly power and load profiles as well as battery storage profiles of the recommended Case 3 and Case 5, respectively. The largest PV areas and battery capacity adopted in Case 3 will contribute to an optimal selection based on multi-dimensional assessment considering both the energy and economic performance, while the smallest PV areas without battery participation adopted in Case 5 contribute to an optimal selection based on economic evaluation. The comparison results indicate that the renewable power generation in Case 3 is 2.5–3 times higher than renewable power

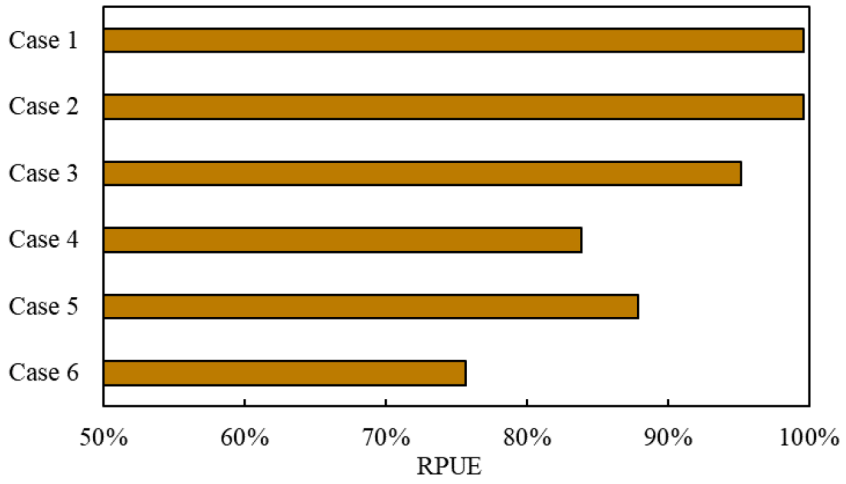

Fig. 8. Quantification results of RPUE among these six cases.

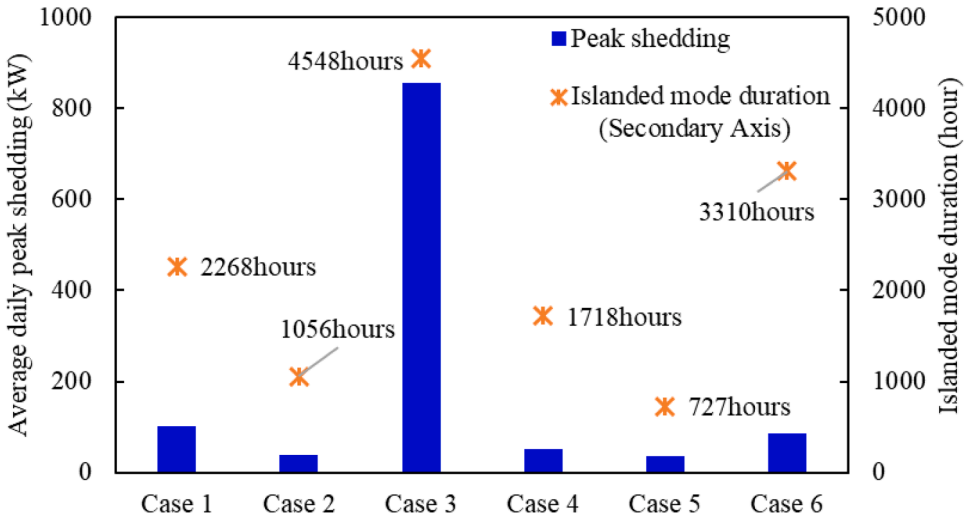

Fig. 9. Quantification results of the peak shedding and islanded mode duration among these six cases.

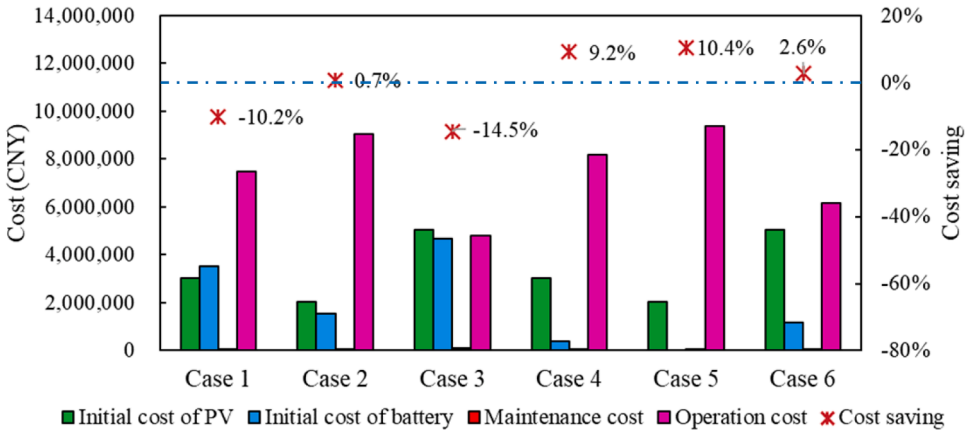

Fig. 10. Assessment and comparison results of the system economic performance among these six optimization cases.

generation in Case 5. The battery plays a negligible role in Case 5 as the peak radiation happens. That means, there are still divergences in the optimization paths of energy and economic aspects.

4.7. In-depth examination of the multi-functional building complex with PV power generation

For the programs with small-fluctuated electricity power consumption throughout the 24 h, the potential of the solar multi-functional

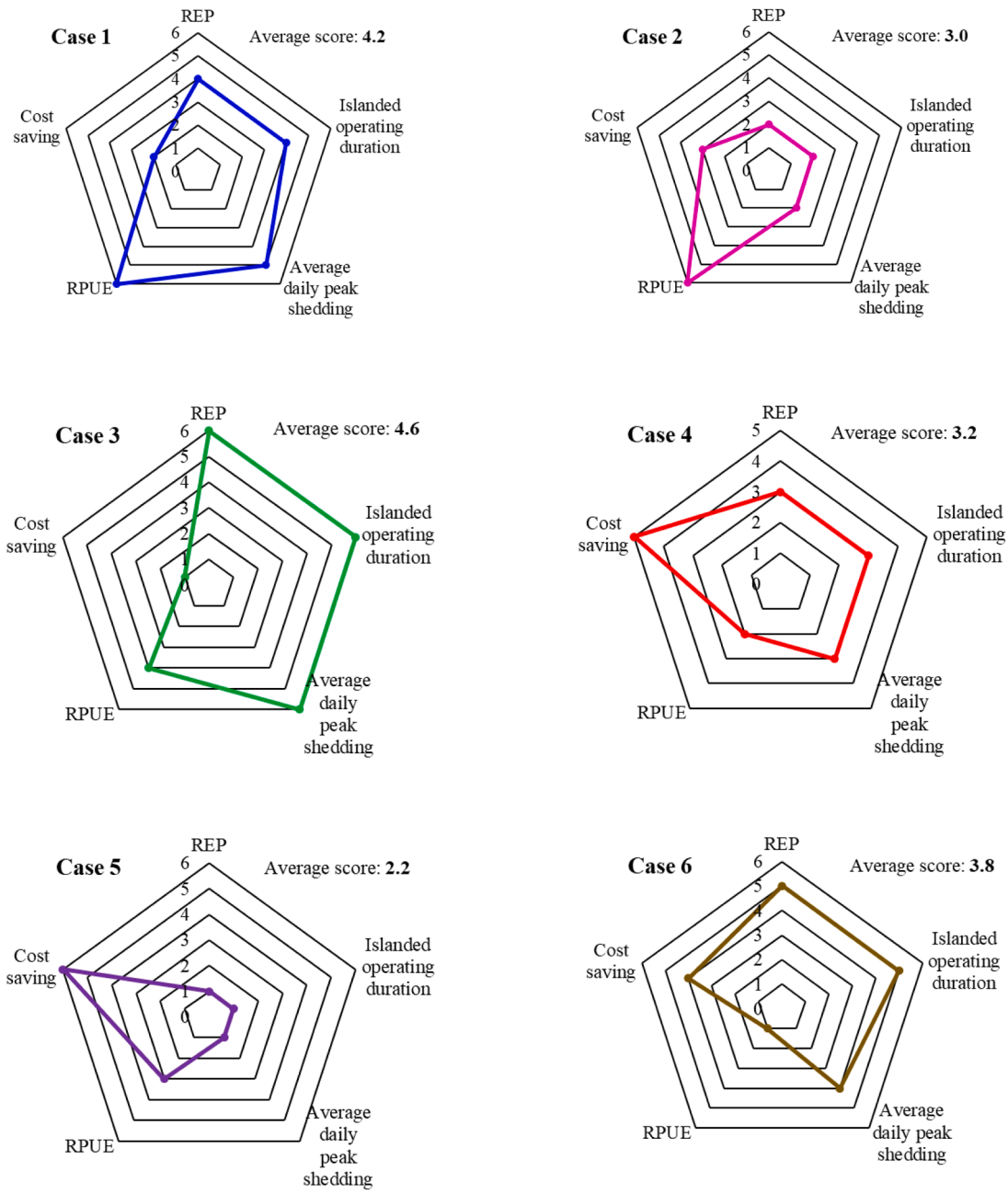

Fig. 11. Multi-dimensional performance comparison concerning these six optimization cases.

building complex is explored and the techno-economic comparative assessment is discussed varying the matching strategy of PV area and battery capacity. It is apparent that one still has to sacrifice economic efficiency if one wants to further utilize photovoltaic and battery energy storage technologies to achieve energy-saving and emission reduction goals. Based on the current development status of PV and battery energy storage, it is highly recommended to increase investment in PV and battery energy storage in regions with renewable energy subsidies. Obviously, from the perspective of project investors, large-scale PV and battery energy storage still need to overcome funding problems. Therefore, further efforts still need to be made on the technical breakthroughs in renewable energy systems and market optimization.

For this study, the pursuit of enhanced energy performance in the solar-powered multifunctional building complex often presents trade-offs with economic gains, as evidenced in Cases 3 and Case 5. The average scores of the system performance in Cases 3 and Case 5 are 4.6 and 2.2, respectively. The comparison results show that battery storage is a valuable technology for improving the utilization of renewable energy, the associated upfront costs and the impact of battery capacity on overall system expenses must be carefully evaluated in the context of system optimization. Achieving a balanced scenario where both energy efficiency and economic viability coexist is essential, particularly in light of the diverse functionalities within the building complex.

5. Discussion

5.1. Discussion of the methodology

Some typical assessment methods like multi-criteria decision making (MCDM), multi-attribute utility theory (MAUT) and so on, have been tested and validated in the previous studies for the energy system assessment concerning different objectives. MCDM is a branch of

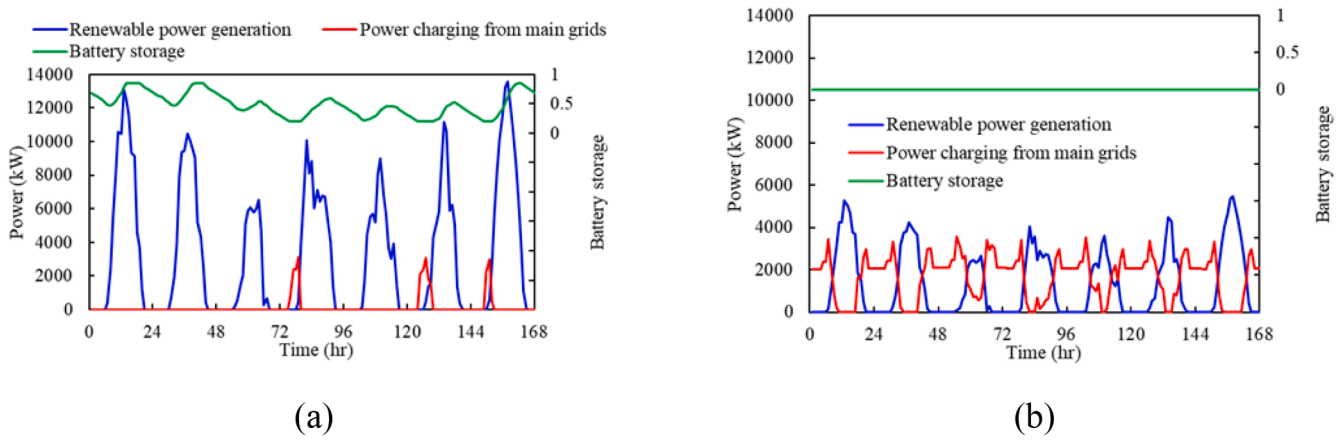

Fig. 12. Weekly power and load profiles as well as battery storage profiles for recommended Case 3 (a) and Case 5 (b).

operations research and management science that provides decision-makers with a structured methodology to evaluate, rank, and select among a finite set of alternatives under multiple (often conflicting) criteria. For instance, Moradi et al. [50] applied the MCDM analysis to assess renewable energy options in Algeria, taking into account both economic and environmental factors. Hosouli and Hassani [51] developed a multi-criteria decision making (MCDM) model to select the solar plant location considering several factors including temperature, annual hours of sunshine, absolute humidity, proximity to major roads, distance from the power network, and potential demand. As for the developed innovative multi-dimensional performance comparison and the average score of the system performance, it ventures a novel method to contribute to the multi-objective domain for the multi-dimensional performance of the energy system. Evaluated through a case study, we hope this modest contribution may offer insights for subsequent evaluation frameworks. The highest average score (Case 3) and the largest cost saving (Case 5) are further analyzed and discussed in the assessment as shown in Section 4.6.

5.2. Discussion of the target energy system

In this work, the target energy system is a typical multi-functional building complex including 10 different buildings in three different areas (cargo area, living area and office area). To better ground the proposed evaluation method in practical applications, it is necessary to consider and apply it to other types of multi-functional building complexes. Progress should be made in the following aspects:

- Clarifying the load composition of different types of multi-functional building complexes and establishing reasonable simulations;
- Evaluating photovoltaic power generation based on local climatic conditions;
- Conducting a comprehensive quantification of the economic performance of the entire system according to local hardware cost levels;
- Conducting the performing assessment calculations using our proposed methodology. Also, this approach should also be integrated with other research to enable a more comprehensive evaluation and analysis.

6. Conclusions and future studies

This paper proposed a novel techno-economic assessment framework for the multi-functional building complex energy system integrated with photovoltaic systems. According to the comparative assessment and analysis results, the main findings can be concluded as follows:

- The developed techno-economic comparative assessment can effectively quantify the system performance. The results confirm the workability of the proposed framework that effectively provides valuable support and guidance in the system design for the decision-makers and/or system designers and the recommended design cases (Case 3 and Case 5) are obtained considering the highest average score at 4.6 and maximum cost saving at 10.4 %, respectively.
- The dynamic load consumption, taking into account the specific and different characteristics of building functions and schedules, is thoroughly quantified and analyzed. A method of load calculation based on the coupling of fixed loads and dynamic loads over a 24-hour cycle enables comprehensive load quantification for multi-functional complexes like cargo terminals.
- Employing design optimization to maximize the REP and minimize the LCOE, the optimal battery capacities are obtained under determined PV areas. The maximum REP is up to 60 % when the largest PV area is equipped with a battery capacity of 87.94 MWh and the minimum LCOE is obtained at 0.49 CNY/kWh (0.0680 US$/kWh) when the smaller PV area at 40,756 m^2 without the battery storage participation is adopted.
- Multi-dimensional performance assessment and comparison have been performed to identify the recommended case. An innovative scoring mechanism is first developed and introduced in the system multi-dimensional performance assessment, which is used to conduct the comparison for those cases. The recommended case is obtained, which has overall benefits over the baseline case scenario although the score in one dimension cannot be satisfactory.

Future research should expand this framework by integrating additional renewable technologies like wind or geothermal alongside solar PV, exploring advanced battery chemistries and thermal storage solutions, and implementing machine learning algorithms for energy demand forecasting and system control optimization. The influence of different tariff structures such as time-of-use (TOU), critical peak pricing (CPP), and demand charges is indispensable for an accurate economic assessment. Consequently, a detailed quantification of their impact on the system's economic performance will be incorporated into our future work, based on the actual conditions of the project. Furthermore, incorporating life cycle assessment to evaluate environmental impacts, examining how regulatory frameworks influence system adoption, and modeling resilience during grid outages would enhance our understanding of these complex energy systems. These advancements will collectively accelerate the transition toward more sustainable, resilient, and cost-effective urban energy infrastructure while providing valuable insights for diverse building types across different climate zones and socioeconomic contexts. In the end, as the project moves forward, rigorous validation will indeed be valuable and necessary for refining

the evaluation methodology. This important step will be addressed in our future work.

CRediT authorship contribution statement

Xuesong Yang: Writing – original draft, Methodology, Investigation, Formal analysis, Conceptualization. **Chao Zeng:** Methodology, Investigation, Formal analysis. **Yushan Yao:** Methodology, Investigation, Formal analysis. **Jianing Luo:** Writing – review & editing, Writing – original draft, Software, Methodology, Investigation, Funding acquisition, Formal analysis, Conceptualization. **Zhengxuan Liu:** Writing – review & editing, Supervision, Software, Methodology, Investigation, Formal analysis, Conceptualization.

Declaration of competing interest

The authors declare that they have no known competing financial interests or personal relationships that could have appeared to influence the work reported in this paper.

Acknowledgements

The research presented in this study is financially supported by National Natural Science Foundation of China (No.: 52208129); Natural Science Foundation of Sichuan Province (No: 2024NSFSC0915); Natural Science Foundation of Sichuan Province (No: 24NSFSC7156); National Key R&D Program of China (No: 2022YFC3802704); and supported by the Fundamental Research Funds for the Central Universities (No.: A0920502052401–177).

Data availability

Data will be made available on request.

References

[1] D Gielen, F Boshell, D Saygin, MD Bazilian, N Wagner, R Gorini, The role of renewable energy in the global energy transformation, Energy Strategy Rev. 24 (2019) 38–50.
[2] M Shirinbakhsh, LD Harvey, Feasibility of achieving net-zero energy performance in high-rise buildings using solar energy, Energy Built Environ. 5 (2024) 946–956.
[3] D Li, X Cui, L Shi, Y Li, An overview of the research on the correlation between solar energy utilization potential and spatial morphology, Results Eng. 24 (2024) 103444.
[4] JA. Qadourah, Energy and economic potential for photovoltaic systems installed on the rooftop of apartment buildings in Jordan, Results Eng. 16 (2022) 100642.
[5] W Zheng, H He, F Qin, Y Lan, Y Yin, Effect of the overhead height and tilt angle on comprehensive performance of photovoltaic roof based on simulation and experimental methods, Results Eng. 25 (2025) 104292.
[6] V Kapsalis, C Maduta, N Skandalos, M Wang, SS Bhuvad, D D'Agostino, et al., Critical assessment of large-scale rooftop photovoltaics deployment in the global urban environment, Renewable Sustainable Energy Rev. 189 (2024) 114005.
[7] Z Liu, Y Zhou, J Yan, T Marcos, Frontier ocean thermal/power and solar PV systems for transformation towards net-zero communities, Energy 284 (2023) 128362.
[8] H Peng, S Dai, H Liu, Wind loading characteristics and roof zoning of solar arrays mounted on flat-roofed tall buildings, J. Build. Eng. 66 (2023) 105823.
[9] J Luo, H Li, G Huang, S Wang, A multi-dimensional performance assessment framework for microgrids concerning renewable penetration, reliability, and economics, J. Build. Eng. 63 (2023) 105508.
[10] D Lingfors, T Johansson, J Widén, T Broström, Target-based visibility assessment on building envelopes: Applications to PV and cultural-heritage values, Energy Build. 204 (2019) 109483.
[11] RA Mangkuto, DNAT Tresna, IM Hermawan, J Pradipta, N Jamala, B Paramita, Experiment and simulation to determine the optimum orientation of building-integrated photovoltaic on tropical building façades considering annual daylight performance and energy yield, Energy Built Environ. 5 (2024) 414–425.
[12] A Boccalatte, M Fossa, C Ménézo, Best arrangement of BIPV surfaces for future NZEB districts while considering urban heat island effects and the reduction of reflected radiation from solar façades, Renewable Energy 160 (2020) 686–697.
[13] H. Shen, Planning of renewable energy regional heating system based on demand side uncertainty, Results Eng. 22 (2024) 101997.
[14] J Luo, H Li, S Wang, A quantitative reliability assessment and risk quantification method for microgrids considering supply and demand uncertainties, Appl. Energy 328 (2022) 120130.
[15] SØ Jensen, A Marszal-Pomianowska, R Lollini, W Pasut, A Knotzer, P Engelmann, et al., IEA EBC annex 67 energy flexible buildings, Energy Build. 155 (2017) 25–34.
[16] X Luo, T Li, H Wu, Y Wang, Flexibility evaluation and optimal scheduling of flexible energy loads considering association characteristics in residential buildings, Building Simulation: Springer (2025) 1–25.
[17] A Shirole, M Wagh, V Kulkarni, P Patil, Short-term energy scenario of district energy system using optimised renewable energy mix with and without energy storage, Results Eng. 18 (2023) 101017.
[18] A Daghouri, S El Hani, Y El Hachimi, H Mediouni, Enhanced hybrid energy storage system combining battery and supercapacitor to extend nanosatellite lifespan, Results Eng. 23 (2024) 102634.
[19] MJM. Al Essa, Energy assessments of a photovoltaic-wind-battery system for residential appliances in Iraq, J. Energy Storage 59 (2023) 106514.
[20] J Luo, Y Yuan, MM Joybari, X Cao, Development of a prediction-based scheduling control strategy with V2B mode for PV-building-EV integrated systems, Renewable Energy 2024 (2024) 120237.
[21] M Jayachandran, RK Gatla, KP Rao, GS Rao, S Mohammed, AH Milyani, et al., Challenges in achieving sustainable development goal 7: Affordable and clean energy in light of nascent technologies, Sustainable Energy Technol. Assess. 53 (2022) 102692.
[22] X Zhou, S Xue, H Du, Z Ma, Optimization of building demand flexibility using reinforcement learning and rule-based expert systems, Appl. Energy 350 (2023) 121792.
[23] Luo J. Quantitative performance assessment and optimal design of microgrid systems considering supply-demand uncertainties. 2023.
[24] RZ Falama, MD Kaoutoing, FK Mbakop, V Dumbrava, S Makloufi, N Djongyang, et al., A comparative study based on a techno-environmental-economic analysis of some hybrid grid-connected systems operating under electricity blackouts: A case study in Cameroon, Energy Convers. Manage. 251 (2022) 114935.
[25] R Loisel, L Lemiale, Comparative energy scenarios: Solving the capacity sizing problem on the French Atlantic Island of Yeu, Renewable Sustainable Energy Rev. 88 (2018) 54–67.
[26] J Luo, C Zhuang, J Liu, Lai K-h. A comprehensive assessment approach to quantify the energy and economic performance of small-scale solar homestay hotel systems, Energy Build. 279 (2023) 112675.
[27] M Hu, B Zhao, X Ao, X Ren, J Cao, Q Wang, et al., Performance assessment of a trifunctional system integrating solar PV, solar thermal, and radiative sky cooling, Appl. Energy 260 (2020) 114167.
[28] J Luo, X Cao, Y Yuan, Comprehensive techno-economic performance assessment of PV-building-EV integrated energy system concerning V2B impacts on both building energy consumers and EV owners, J. Build. Eng. 2024 (2024) 109075.
[29] X Zhang, F Xiao, Y Li, Y Ran, W Gao, Flexible coupling and grid-responsive scheduling assessments of distributed energy resources within existing zero energy houses, J. Build. Eng. 87 (2024) 109047.
[30] J Luo, MM Joybari, Y Ma, J Liu, Assessment of renewable power generation applied in homestay hotels: Energy and cost-benefit considering dynamic occupancy rates and reservation prices, J. Build. Eng. 2024 (2024) 109074.
[31] C Zeng, J Luo, Y Yuan, F Haghighat, Energy, economic, and environmental (3E) performance assessment, comparison, and analysis of airport cargo terminal microgrid system under the islanded and grid-connected modes, J. Build. Eng. 2023 (2023) 108270.
[32] A Sohani, H Sayyaadi, C Cornaro, MH Shahverdian, M Pierro, D Moser, et al., Using machine learning in photovoltaics to create smarter and cleaner energy generation systems: A comprehensive review, J. Cleaner Prod. 364 (2022) 132701.
[33] DS Pillai, V Shabunko, A Krishna, A comprehensive review on building integrated photovoltaic systems: Emphasis to technological advancements, outdoor testing, and predictive maintenance, Renewable Sustainable Energy Rev. 156 (2022) 111946.
[34] A Arabkoohsar, A Behzadi, AS Alsagri, Techno-economic analysis and multi-objective optimization of a novel solar-based building energy system; An effort to reach the true meaning of zero-energy buildings, Energy Convers. Manage. 232 (2021) 113858.
[35] JT Luo, MM Joybari, K Panchabikesan, F Haghighat, A Moreau, M Robichaud, Parametric study to maximize the peak load shifting and thermal comfort in residential buildings located in cold climates, J. Energy Storage 30 (2020) 101560.
[36] J Luo, K Panchabikesan, Lai K-h, TO Olawumi, MC Mewomo, Z Liu, Game-theoretic optimization strategy for maximizing profits to both end-users and suppliers in building rooftop PV-based microgrids, Energy 313 (2024) 133715.
[37] K. Kusakana, Optimal energy management of a grid-connected dual-tracking photovoltaic system with battery storage: Case of a microbrewery under demand response, Energy 212 (2020) 118782.
[38] S. Abdelhady, Performance and cost evaluation of solar dish power plant: sensitivity analysis of levelized cost of electricity (LCOE) and net present value (NPV), Renewable Energy 168 (2021) 332–342.
[39] ME Zayed, J Zhao, W Li, AH Elsheikh, Z Zhao, A Khalil, et al., Performance prediction and techno-economic analysis of solar dish/stirling system for electricity generation, Appl. Therm. Eng. 164 (2020) 114427.
[40] Liu X, Zeng C, Cao X, Luo J, Yuan Y. Regional Differentiation on Integrated Energy System Performance with Evs in a Pv-Equipped Station-City Complex. Available at SSRN 5293807.
[41] C Zeng, J Luo, Y Yuan, F Haghighat, Energy, economic, and environmental (3E) performance assessment, comparison, and analysis of airport cargo terminal microgrid system under the islanded and grid-connected modes, J. Build. Eng. 82 (2024) 108270.

[42] X Liu, C Zeng, Y Yuan, J Luo, X Lü, F Haghighat, Comprehensive assessment of an integrated energy system with EVs in a PV-equipped station-city complex, Renewable Energy 246 (2025) 122948.
[43] C Zhuang, K Shan, S Wang, Coordinated demand-controlled ventilation strategy for energy-efficient operation in multi-zone cleanroom air-conditioning systems, Build. Environ. 191 (2021) 107588.
[44] J. Luo. Development of Advanced Controller to Achieve Complete Peak Shifting in Light-Weight Residential Buildings Located in Cold Climate, Concordia University, 2019.
[45] Z Liu, J Luo, Y Sun, X Zhang, Z Yan. Advancing urban sustainability: integrating renewable energy for accelerated zero-carbon community transitions, Frontiers Media SA, 2024, p. 1523257.
[46] R Venkateswari, S Sreejith, Factors influencing the efficiency of photovoltaic system, Renewable Sustainable Energy Rev. 101 (2019) 376–394.
[47] P Denholm, J Nunemaker, P Gagnon, W Cole, The potential for battery energy storage to provide peaking capacity in the United States, Renewable Energy 151 (2020) 1269–1277.
[48] H Li, S Wang, Coordinated optimal design of zero/low energy buildings and their energy systems based on multi-stage design optimization, Energy 189 (2019) 116202.
[49] G Psarros, A Papakonstantinou, J Anagnostopoulos, S Papathanassiou, N Boulaxis, Contribution of energy storage to capacity adequacy—Application to island power systems. CIGRE 2020 (2020) 1–10.
[50] B Moradi, M Jahangiri, A Khechekhouche, MSH Mehr, M Nahavandi, Towards Resilient Energy Decisions: Integrating Scenario-Based Weighting and Monte Carlo Sensitivity in Hybrid Renewable System Selection in Algeria, Results Eng. 2025 (2025) 107020.
[51] S Hosouli, RA Hassani, Application of multi-criteria decision making (MCDM) model for solar plant location selection, Results Eng. 24 (2024) 103162.